PHYSICAL REVIEW B VOLUME 50, NUMBER 17 1 NOVEMBER 1994-I

Successive structural phase transitions in a hexagonal linear-chain ferroelectric crystal $RbMnBr_3$

T. Kato, K. Machida, T. Ishii,* and K. Iio
Department of Physics, Faculty of Science, Tokyo Institute of Technology, Oh-okayama, Meguro-ku, Tokyo 152, Japan

T. Mitsui
Department of Physics, Faculty of Pharmaceutical Sciences, Teikyo University, Sagamiko-cho, Tsukui-gun, Kanagawa 199-01, Japan
(Received 15 July 1994)

Birefringence and dielectric measurements were performed on a triangular lattice antiferromagnet $RbMnBr_3$. Successive structural phase transitions at T_4 (~220 K), T_3 (=230 K), and T_2 (=444 K) were found. Through D-E hysteresis loop observations, the phases IV ($T_4<T<T_3$), III ($T_3<T<T_2$), and II ($T_2<T<T_{melt}$) were determined to be ferroelectric. The spontaneous polarization is along the c axis, which disappears abruptly at T_4 with decreasing temperature. Below T_4 (phase V) the crystal is proposed to be antiferroelectric. The dielectric behavior of $RbMnBr_3$ is very similar to that of $KNiCl_3$; however, a higher-temperature phase transition at T_1 assigned for $KNiCl_3$ was not detected in differential-scanning-calorimetry data on $RbMnBr_3$.

I. INTRODUCTION

Recent dielectric studies of $KNiCl_3$ (Ref. 1) and $RbFeBr_3$ (Ref. 2) revealed that so-called $KNiCl_3$-type hexagonal linear-chain crystals with space group $P6_3cm$ are ferroelectric. The present report on $RbMnBr_3$ describes one of our continuing studies of the successive structural phase transitions accompanied by ferroelectricity in crystals of the "$KNiCl_3$ family" ($KNiCl_3$, $RbFeBr_3$, and $RbMnBr_3$).

Magnetic phase transitions in those crystals have aroused much interest as they exhibit characteristics of the partially released spin frustration on a triangular lattice with distortion.[3–5] In the fully frustrated XY spin systems without distortion, such as $CsMnBr_3$, the magnetic ordering at the Néel point T_N without an in-c-plane magnetic field ($H=0$) is tetracritical, which is characterized by the critical exponents of the chiral "$Z_2\times S_1$" universality class.[6] Application of the magnetic field induces a splitting of T_N so as to produce a magnetic intermediate phase.[7] This knowledge has recently been established theoretically and experimentally. On the other hand, it has been noted as a new viewpoint that an appropriate distortion introduced to the triangular lattice also makes the magnetic phase transition successive.[8,9] Then it is possible to touch experimentally on a virtual region of $H^2<0$ in a theoretical H–T phase diagram.[7] The magnetic phase diagram of $RbMnBr_3$, a slightly distorted triangular lattice antiferromagnet, was recently clarified by neutron diffraction.[10,11] Contrary to the expectation that the magnetic phase transition of $RbMnBr_3$ without the field can be successive as those of $RbFeBr_3$ (Ref. 4) and $RbVBr_3$ (Ref. 5) are, $RbMnBr_3$ has a single ordering point at T_N. Furthermore, an incommensurate spin structure of $RbMnBr_3$, of which the origin has long been unclear, was found to transform into a commensurate structure by applying the in-c-plane field.[11] To understand fairly complex magnetic phase transitions in these distorted triangular lattice systems, detailed information on the structures must be sought.

The prototype structure of the $KNiCl_3$ family crystals is the well-known "$CsNiCl_3$-type" structure with nonpolar $P6_3/mmc$ symmetry, characterized as $(NiCl_3)^-$ linear chains of face-sharing octahedra. At room temperature (RT), $RbMnBr_3$ takes a modified structure with $P6_3cm$ symmetry,[12] which is called "$KNiCl_3$-type" structure because the first analysis of this type was performed in $KNiCl_3$ at RT.[13,14] Since two-thirds of the $(MnBr_3)^-$ chains are shifted along the c axis and one-third of the chains are shifted in the antiparallel direction, the crystal is permitted to be ferrielectric. A freezing of K_4 mode lattice vibrations of the prototype $CsNiCl_3$ structure is proposed to be responsible for this structure.[15] Compatibility relations permit the coexistence with A_{2u} mode distortion, which induces a spontaneous polarization parallel to the c axis.

Our recent experimental findings of ferroelectricity in $KNiCl_3$ and $RbFeBr_3$ will stimulate studies on the structural phase transitions in the hexagonal ABX_3 compounds with $(BX_3)^-$ linear chains, and also on the magnetoelectric properties in the distorted triangular lattice antiferromagnets. The present study aims to characterize the successive structural phase transitions in $RbMnBr_3$ through optical birefringence and dielectric measurements.

II. EXPERIMENTAL PROCEDURES AND RESULTS

Single crystals of $RbMnBr_3$ (Ref. 3) were grown by the vertical Bridgman method. To prepare c-plate samples, a few pieces of crystals with c planes were selected after the crystals were cut with a knife. A sanding process[3] was not employed to avoid introducing microcracks. By cleaving, ac-plate samples were easily obtained.

From now on, we use the prototype $CsNiCl_3$-type structure to define the primitive lattice. Then, a unit cell of the RT structure becomes $\sqrt{3}a\times\sqrt{3}a\times c$. A cleavage plane is the ac plane, normal to the a^* axis.[10] The birefringence Δn^{ac} for light propagating perpendicular to the c axis indicates the difference between principal indices n_c and n_a. Nevertheless, from a measurement of electric capacitance of the cleaved ac plate, we show the dielectric constant as ε_a for

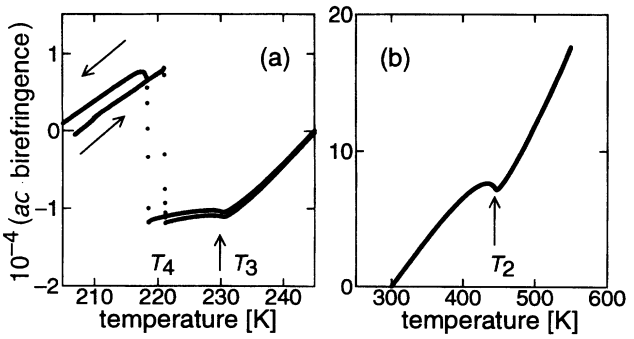

FIG. 1. The ac-plane birefringence of $RbMnBr_3$ (a) around T_4 ($\sim$220 K) and T_3 (=230 K) measured relatively from T=245 K and (b) around T_2 (=444 K) from T=300 K. T_4 indicates the first-order phase transition with thermal hysteresis of about 5 K (218$\sim$223 K).

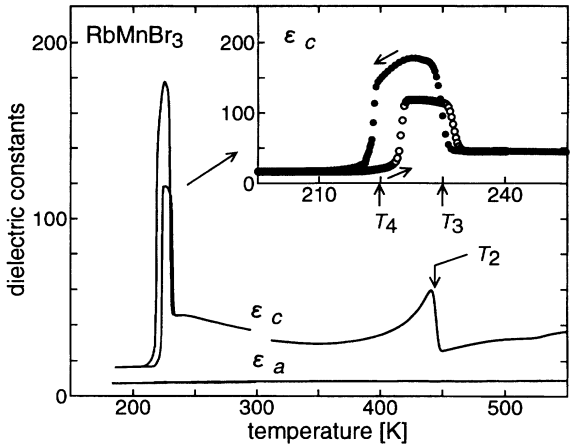

FIG. 2. Temperature dependence of dielectric constants ε_c and ε_a of $RbMnBr_3$, which were obtained from measurements of capacitance of the c and the cleaved ac plates, respectively.

convenience. Temperature detection was performed through an AuFe-chromel thermocouple for $T<$RT or a chromel-alumel thermocouple for $T>$RT.

The temperature dependence of the ac-plane birefringence $\Delta n^{ac}(T)$ at λ=632.8 nm is measured, as shown in Fig. 1, which is complementary to the data shown in Ref. 3. The rotating-analyzer method[16,17] was used for the birefringence measurement. Anomalies at $\sim$220 K ($=T_4$) of the first-order phase transition accompanied by a thermal hysteresis of about 5 K, and at 230 K ($=T_3$) and 444 K ($=T_2$) of the second-order transitions are clearly seen. At lower temperatures below T_4 ($=T_{S2}$ in Ref. 3), $\Delta n^{ac}(T)$ of $RbMnBr_3$ exhibits an anomaly solely at the magnetic ordering temperature T_N =8.5 K.[3]

We also performed an optical-microscope observation for the c plate. The c-plate sample was chosen thus that the conoscopic pattern for the uniaxial crystal was observable at RT. At T_4, twin layers appear in the c plane in cooling and disappear in heating. The twinning patterns are different in each observation in cooling. The typical thickness of the layer was roughly estimated to be $\sim$3 μm. The conoscopic pattern disappears below T_4 because the incident light is scattered. The optical anisotropy below T_4 in the c plane was also confirmed through the averaged c-plane birefringence Δn^c for light propagating along the c axis, where the value Δn^c below T_4 is not reproducible.

Next, the dielectric constants were measured by means of a low-frequency impedance analyzer (HP 4192A) at a frequency of 1 MHz. For the electrodes silver paste was used. The representative dimensions of the samples were 10 $mm^2 \times 1.5$ mm. The temperature dependences of ε_c and ε_a of $RbMnBr_3$ are shown in Fig. 2. In this figure the traces above 300 K are of heating measurements, and those below 300 K are of successive cooling and heating measurements. Anomalies associated with the structural phase transitions at T_4, T_3, and T_2 were observed only in ε_c. Thermal hysteresis was observed at T_4. The ε_c measurement at lower temperatures down to $\sim$11 K revealed that meaningful change does not appear below $\sim$200 K. Data above T_2, especially around $T=\sim$535 K, were not reproducible. At such high temperatures, the dielectric loss ($=\tan\delta$) became larger with heating. The loss was negligible at temperatures near to 300 K; however, at the temperatures around T_4 and T_3, the loss for the c plate showed a slight increase.

Figure 3 shows the representative 50 Hz D–E hysteresis loops observed by use of the conventional Sayer-Tower circuit. Obtained values of coercive field E_c and spontaneous polarization P_s are 1.17 kV/cm and 3.8 μC/cm^2 at 470 K (in phase II), 0.071 kV/cm and 0.0032 μC/cm^2 at 243 K (III),

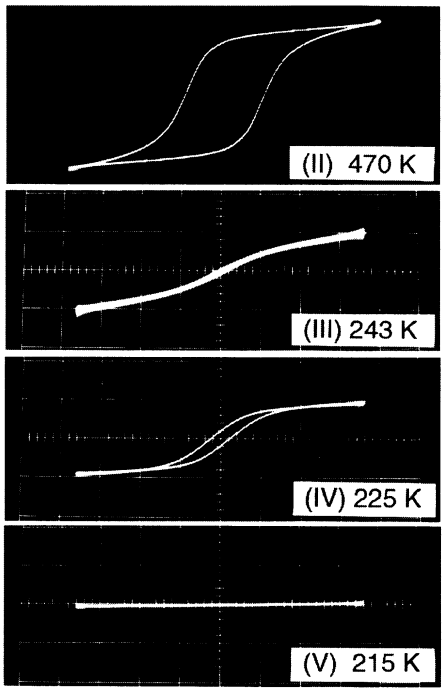

FIG. 3. The representative 50 Hz D–E hysteresis loops for c-plate samples of $RbMnBr_3$. Coercive fields E_c and spontaneous polarization P_s obtained from this figure are 1.17 kV/cm and 3.8 μC/cm^2 for 470 K (phase II), 0.071 kV/cm and 0.0032 μC/cm^2 for 243 K (III), and 0.082 kV/cm and 0.030 μC/cm^2 for 225 K (IV), respectively. Neither is detectable for 215 K (V). The maximum values of applied electric field E_{max} are 4.60 kV/cm for phase II and 1.25 kV/cm for III–V.

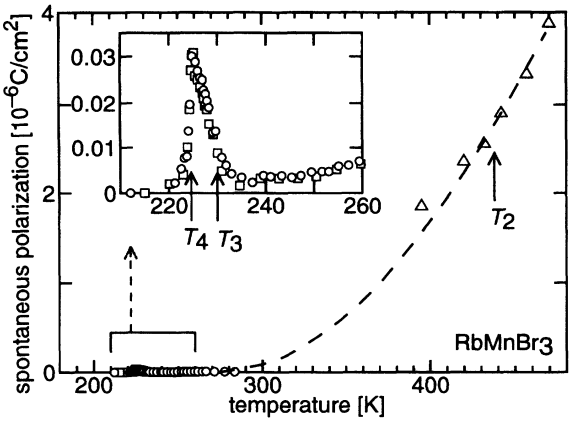

FIG. 4. Temperature dependence of the spontaneous polarization P_s of $RbMnBr_3$ obtained from the D–E hysteresis loops in heating measurements. Circles, squares, and triangles represent different samples.

and 0.082 kV/cm and 0.030 $\mu C/cm^2$ at 225 K (IV), respectively. Neither is detectable at 215 K (V). It should be noted that the maximum intensity of applied electric field E_{max} is small (4.60 kV/cm for phase II and 1.25 kV/cm for phases III–V). The dielectric loss appeared compensated enough to present the saturation of the loop at higher fields. The temperature dependence of the spontaneous polarization $P_s(T)$ measured up to 511 K is plotted in Fig. 4. $P_s(T)$ in $RbMnBr_3$ is very similar to that of $KNiCl_3$;[1] $P_s(T)$ is zero in phase V, rather large in phase IV, and nonzero but very small in III, but drastically increases at temperatures near T_2 (III→II). Through such observations, three phases IV ($T_4<T<T_3$), III ($T_3<T<T_2$), and II ($T_2<T$) of $RbMnBr_3$ are determined to be ferroelectric.

From these results, the structural phase transition points of $RbMnBr_3$ are summarized in Fig. 5, where those of $KNiCl_3$ (Ref. 1) are referred to for comparison. The dielectric properties in the successive phase transitions of the two types of crystals are very similar. However, a question arises as to whether or not the higher-temperature phase transition (T_1 of $KNiCl_3$; the first order) above T_2 also exists in $RbMnBr_3$. The anomaly at 535 K in the temperature dependence of ε_c might suggest the presence of T_1. To examine it, differential-scanning-calorimetry measurements of powdered crystals of about 40 mg in an aluminum cell were performed by use of the calorimeter of Perkin-Elmer DSC-7. No

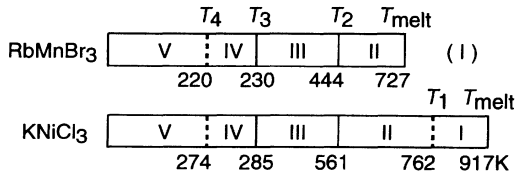

FIG. 5. Phase transition point lists of $RbMnBr_3$ and $KNiCl_3$. Temperatures for $RbMnBr_3$ are from the present study, and those for $KNiCl_3$ are from Ref. 1. The broken lines indicate the first-order phase transitions, and the solid lines indicate the second-order ones. The prototype phase I for $RbMnBr_3$ is hypothesized to be above the melting point.

anomalies were observed in the scans repeated several times in a temperature range between RT and 630 K. In the first heating above 630 K, only melting point $T_{melt}=727$ K was detected. However, once the samples were heated above ~630 K, extra anomalies at 535.7, 599.3, 712.6, and 719.6 K were observed, which indicate the synthesis of RbBr-rich compounds[18] such as Rb_2MnBr_4. Thus the first-order transition in pure $RbMnBr_3$ does not exist above T_2.

III. DISCUSSION

From the hysteresis in the D–E loops, at temperatures between T_4 and T_{melt}, $RbMnBr_3$ is found to be a ferroelectric crystal in which P_s is parallel to the c axis. The temperature dependence of P_s of $RbMnBr_3$ shows quite unusual behavior; however, it resembles that of $KNiCl_3$.[1] A possible interpretation for the $P_s(T)$ in phase III is that the observed saturation is a central loop of the triple hysteresis loops in ferrielectrics.[19] Since the reported crystal structure in the RT phase III is of the $KNiCl_3$ type, the simplest model for its ferroelectricity is that all chains become polar and align ferrielectrically on a basal-plane triangular lattice. The virtual ferroelectric Curie temperature of $RbMnBr_3$ is thought to be very high; thus at RT the complete saturation of $P_s(E)$ is rarely observed. Phase II in $KNiCl_3$ and $RbMnBr_3$, in which the spontaneous polarization was found to be rather large, is expected to be a ferroelectric phase with $a\times a\times c$ unit cells from supergroup-subgroup relations of symmetry considerations.[1] At near T_2 in the heating run, the apparent increase of P_s must be due to the change from the D–E triple loop to a single one. It is interesting to compare this with the fact that a related crystal $RbFeBr_3$ exhibits a typical paraelectric-ferroelectric phase transition at the Curie temperature $T_C=34.4$ K, below which the structure is reported to be of the $KNiCl_3$ type.[2]

Below T_4 (phase V) in $RbMnBr_3$, P_s vanishes completely. A single-crystal x-ray diffraction study on phase V of this crystal[20] revealed that $RbMnBr_3$ at $T=200$ K is a commensurate structure with a long period ($4\sqrt{3}a\times 4\sqrt{3}a$) in the basal plane, where the anisotropy in the c plane was not detected. Phase V may be regarded as paraelectric; however, we can presume that in phase V the polar chains are aligned antiferroelectrically[21] in the c plane. The D–E loops in phase V are evidence enough to understand that only the central part of the triple loops in phase III is suppressed. The D–E loop observations with higher electric fields will be reexamined.

By electron diffraction, Visser and Prodan[14] showed that the $KNiCl_3$ structure at RT has considerable crystal disorder, giving weak reflections with orthorhombic symmetry. The model suggested by them, which is illustrated with a figure in their report, is similar to antiphase boundaries in a long-period hexagonal system.[22] Parallel lines of antiphase boundary in the basal plane of $KNiCl_3$ and $RbMnBr_3$ can be present in a homogeneous polar domain, as observed in a ferroelectric crystal β'-GMO [$Gd_2(MoO_4)_3$].[23] It must be pointed out that since T_3 of $KNiCl_3$ is near to RT, ambiguity remains on the phase (III or IV) in their measurements. Luminescence studies[24–26] showed recently that there are considerable amounts of crystal defects in the $CsNiCl_3$-type crystals. Ramaz, Vial, and Macfarlane[24] and Wolfert and

Blasse[25] have suggested that stacking faults in the sequence of $CsCl_3$ layers, which is of the hexagonal-close-packing type for regular crystals, might be important for the structural phase transitions in $KNiCl_3$, though they have not clarified how the defaults are related to them.

Finally, a comment should be made about the recent neutron-scattering study of $RbMnBr_3$,[11] in which the presence of a nonmagnetic commensurate Bragg peak below about 10 K was reported. This was not detected in neutron scattering performed by a different group[10] including one of the authors (T.K.). Furthermore, no anomaly was detected at such temperatures in the present birefringence measurement.

ACKNOWLEDGMENTS

This study was supported in part by a Grant-in-Aid for Scientific Research from the Ministry of Education, Science and Culture. We thank Professor H. Tanaka for valuable discussions.

*Present address: NEC Corp., Kawasaki, Kanagawa, Japan.

[1] K. Machida, T. Mitsui, T. Kato, and K. Iio, Solid State Commun. **91**, 17 (1994).

[2] T. Mitsui, K. Machida, T. Kato, and K. Iio, J. Phys. Soc. Jpn. **63**, 839 (1994).

[3] T. Kato, K. Iio, T. Hoshino, T. Mitsui, and T. Tanaka, J. Phys. Soc. Jpn. **61**, 275 (1992).

[4] K. Adachi, K. Takeda, F. Matsubara, M. Mekata, and T. Haseda, J. Phys. Soc. Jpn. **52**, 2202 (1983).

[5] H. Tanaka, T. Kato, K. Iio, and K. Nagata, J. Phys. Soc. Jpn. **61**, 3292 (1992).

[6] H. Kawamura, J. Phys. Soc. Jpn. **61**, 1299 (1992).

[7] M. L. Plumer and A. Caillé, Phys. Rev. B **44**, 4461 (1991).

[8] G. Parker, W. M. Saslow, and M. Gabay, Phys. Rev. B **43**, 11 285 (1991).

[9] M. L. Plumer and A. Caillé, Phys. Rev B **45**, 12 326 (1992).

[10] T. Kato, T. Ishii, Y. Ajiro, T. Asano, and S. Kawano, J. Phys. Soc. Jpn. **62**, 3384 (1993).

[11] L. Heller, M. F. Collins, Y. S. Yang, and B. Collier, Phys. Rev. B **49**, 1104 (1994).

[12] H. Fink and H.-J. Seifert, Acta Crystallogr. B **38**, 912 (1982).

[13] D. Visser, G. C. Verschool, and D. J. W. Ijdo, Acta Crystallogr. B **36**, 28 (1980).

[14] D. Visser and A. Prodan, Phys. Status Solidi A **58**, 481 (1980).

[15] J. L. Mañes, M. J. Tello, and J. M. Pérez-Mato, Phys. Rev. B **26**, 250 (1982).

[16] D. E. Aspnes and A. A. Studna, Appl. Opt. **14**, 220 (1975).

[17] T. Nishino, K. Iio, and K. Nagata, J. Spectrosc. Soc. Jpn. **29**, 263 (1980).

[18] Von H.-J. Seifert and G. Flohr, Z. Anorg. Allg. Chem. **436**, 244 (1977).

[19] Y. Shiroishi and S. Sawada, J. Phys. Soc. Jpn. **46**, 148 (1979).

[20] T. Kato and M. Isobe (unpublished).

[21] T. Yamaguchi, S. Sawada, M. Takashige, and T. Nakamura, Jpn. J. Appl. Phys. **21**, L57 (1982).

[22] M. Hirabayashi, S. Yamaguchi, K. Hiraga, N. Ino, H. Sato, and R. S. Toth, J. Phys. Chem. Solids **31**, 77 (1970).

[23] J. R. Barkley and W. Jeitschko, J. Appl. Phys. **44**, 938 (1973).

[24] F. Ramaz, J. C. Vial, and R. M. Macfarlane, Europhys. Lett. **22**, 217 (1993).

[25] A. Wolfert and G. Blasse, J. Solid State Chem. **55**, 344 (1984).

[26] C. Andraud, F. Pellé, and O. Pilla, J. Phys. (Paris) Colloq. **46**, C7-489 (1987).

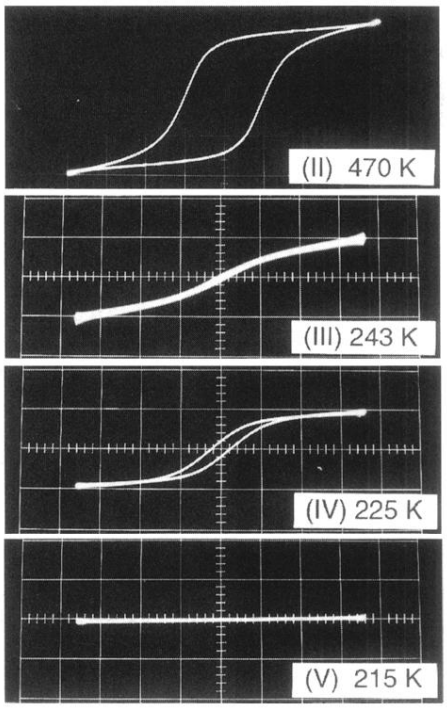

FIG. 3. The representative 50 Hz D–E hysteresis loops for c-plate samples of $RbMnBr_3$. Coercive fields E_c and spontaneous polarization P_s obtained from this figure are 1.17 kV/cm and 3.8 $\mu C/cm^2$ for 470 K (phase II), 0.071 kV/cm and 0.0032 $\mu C/cm^2$ for 243 K (III), and 0.082 kV/cm and 0.030 $\mu C/cm^2$ for 225 K (IV), respectively. Neither is detectable for 215 K (V). The maximum values of applied electric field E_{max} are 4.60 kV/cm for phase II and 1.25 kV/cm for III–V.